Research Support Officer in Quantum Thermodynamics of Precision in Electronic Devices

Applicant: Mr. Ilia Khomchenko
Prospective Research Advisor: Dr. Tony J. G. Apollaro

University of Malta

March 22, 2024

Academic background

Novosibirsk State University, Novosibirsk, Russia,

- **Physics – Bachelor of Science**, GPA: 4.98 out 5.00;

Skolkovo Institute of Science and Technology, Moscow, Russia,

- **Energy systems – Master of Science**, GPA: 4.88 out 5.00.

Skolkovo Institute of Science and Technology, Moscow, Russia, & University of Insubria, Como, Italy, (cotutelle)

- **Physics and Astrophysics – Doctor of Philosophy**,
- **Engineering systems – Doctor of Philosophy**,
- Thesis title: **Energy and Information Management in Superconducting Nanodevices: A Thermodynamic Approach**
- Tentative Defense: June (Second Half), 2024; September 2024.

Industrial and research experience

- Research work: Institute of Thermophysics of Siberian Branch of Russian Academy of Science, Novosibirsk, Russia (2016-2018)
  "Modelling fluid flows in tubes and plane channels"
- Industrial immersion: TION, Novosibirsk, Russia (June-July 2019)
  "Development of a smart residential climate control system"
- Academic mobility: University of Insubria (October-December 2019)
  "Thermodynamic and transport properties of electron gases for energy applications"
- Research Intern, Center of Energy Science and Technology (CEST), Skoltech (August-October 2020)
  "SQUID-based interferometric accelerometer"

Industrial and research experience

- Ph.D. student: Istituto Nazionale di Fisica Nucleare, Milan, Italy (2020-Present)
  "Quantum Thermodinamics of Superconductors"
- Visiting Ph.D. student: University of Genova, Genova, Italy (June 2023)
  "Non-equilibrium resources for nanoscale energy management"

Publications

- **I. Khomchenko**, H. Ouerdane, G. Benenti, "Influence of the Anderson Transition on Thermoelectric Energy Conversion in Disordered Electronic Systems", **IOP Journal of Physics: Conference Series 2701**, 012018 (2024).

- **I. Khomchenko**, P. Navez, H. Ouerdane, "SQUID-based interferometric accelerometer", **Applied Physics Letters 121**, 152601 (2022).

- **I. Khomchenko**, H. Ouerdane, G. Benenti, "Voltage-amplified heat rectification in SIS junctions", **Physical Review B 106**, 2022.

- **I. Khomchenko**, et al., "The thermoelectric conversion efficiency problem: Insights from the electron gas thermodynamics close to phase transition" **SciPost Physics**, under second round of review (arXiv:2110.11000).

Conferences

- EUCAS 2023, 16th European Conference on Applied Superconductivity, Bologna, Italy, (3-7 September, 2023);
  Oral presentation: **I. Khomchenko**, P. Navez, H. Ouerdane.
  SQUID-based interferometric accelerometer.

- 12th International Conference on Mathematical Modelling in Physical Sciences m^2 Physical Sciences, Belgrade, Serbia (28-31 August, 2023);
  Oral presentation: **I. Khomchenko**, H. Ouerdane, G. Benenti.
  Influence of the Anderson Transition on Thermoelectric Energy Conversion in Disordered Electronic Systems.

- QTD 2023, Quantum Thermodynamics 2023, Vienna, Austria (17-21 July, 2023);
  Oral presentation: **I. Khomchenko**, H. Ouerdane, G. Benenti.
  Voltage-amplified heat rectification in SIS junctions.

Hackathons

- QRise 2024, Quantum Research and Industry Skills Exchange, Sanford, USA, (online), (March 4 – April 12, 2024);
- QHack 2024, Quantum Hackathon from Xanadu, Toronto, Canada (online), (16-22 February, 2024);
- iQuHack 2024, MIT's Quantum HACKathon (16^{th} place out 63 in IonQ's challenge), Boston, USA, (online), (2-4 February, 2024).

Doctoral Research

Voltage-amplified Heat Rectification in SIS Junctions

Heat rectification is a process where thermal transport along one axis depends on the sign of the temperature gradient or heat current.

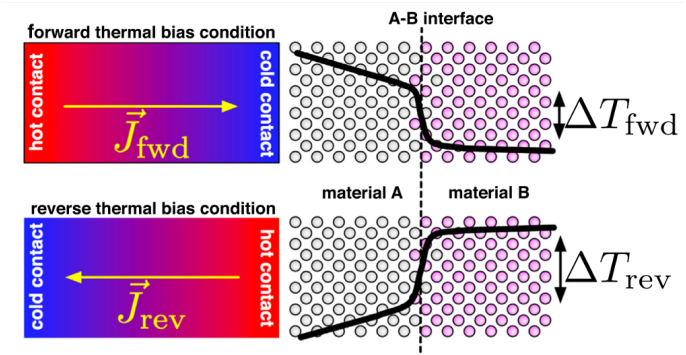

(a) Heat rectification: $J_{\rm fwd} \neq J_{\rm rev}$ [1].

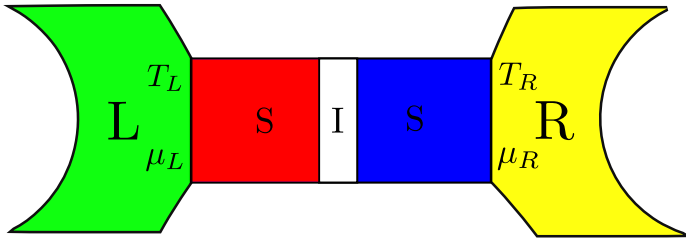

(b) Schematic representation of a SIS junction coupled to the reservoirs.

Figure 1: Heat Rectification in Normal Metals and Superconductors.

[1] R. Dettori et al., J. Appl. Phys. **119**, 215102 (2016).

Voltage-amplified Heat Rectification in SIS Junctions

$$\mathcal{R} = \frac{\dot{Q}_{\rm fw}}{\dot{Q}_{\rm bw}} \quad - \text{ rectification coefficient}$$

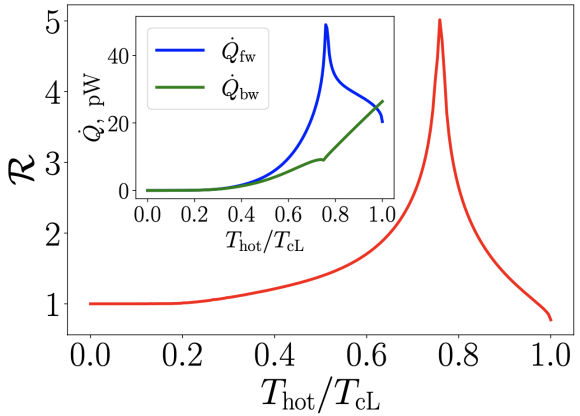

(a) Adiabatic regime:
$V_s(t) = V_0 \sin(\Omega t)$.

$eV_0 \ll \Delta$ and $\hbar\Omega \ll \Delta$
– adiabatic regime

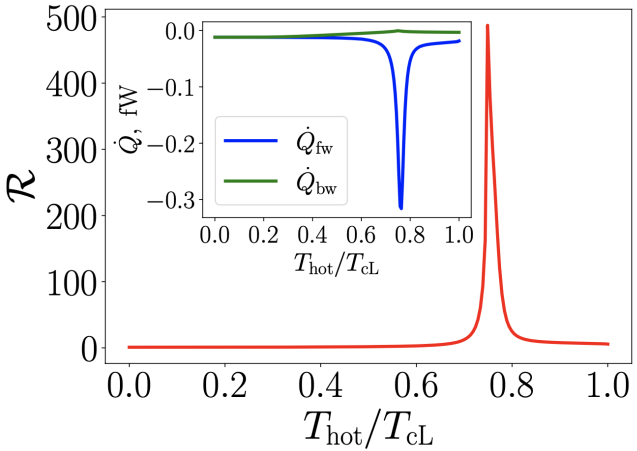

(b) Beyond adiabatic regime:
$V(t) = V_s(t) + V_r(t)$.

Figure 2: Heat Rectification under an Applied Oscillating Voltage [2].

[2] I. Khomchenko, H. Ouerdane, G. Benenti, Phys. Rev. B **106**, 245413 (2022).

Acceleration detection

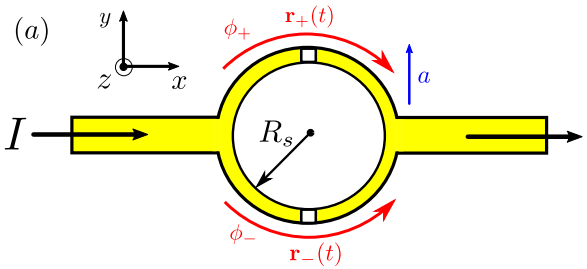

(a) Representation of a SQUID with a ring geometry.

$$\delta\phi = 4mR_s^2 I/(\hbar v)\frac{a}{I}$$

$$f = 4mR_s^2 I/(\hbar v)$$

$$S_a^{1/2} = 4.6{\cdot}10^{-10}\mathrm{m}\cdot\mathrm{s}^{-2}/\sqrt{\mathrm{Hz}}$$

$$a = 4\sqrt{I_c(2I_c - I)}/f$$

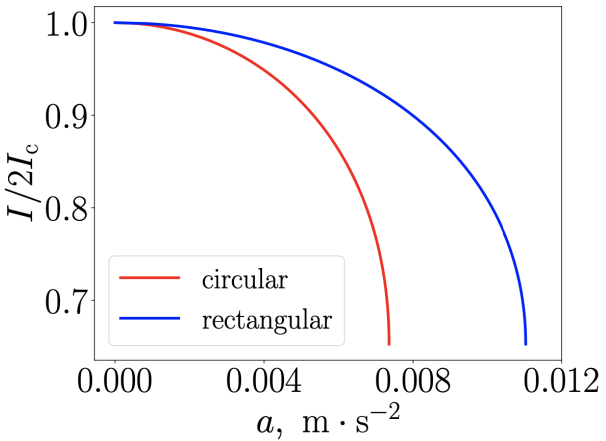

(b) Relative current variation $I/2I_c$ in each arm as function of acceleration a.

Figure 3: SQUID-based interferometric accelerometer [3].

[3] I. Khomchenko, P. Navez, H. Ouerdane, "SQUID-based interferometric accelerometer", Appl. Phys. Lett. **121**, 152601 (2022).

Oscillatory motion measurement

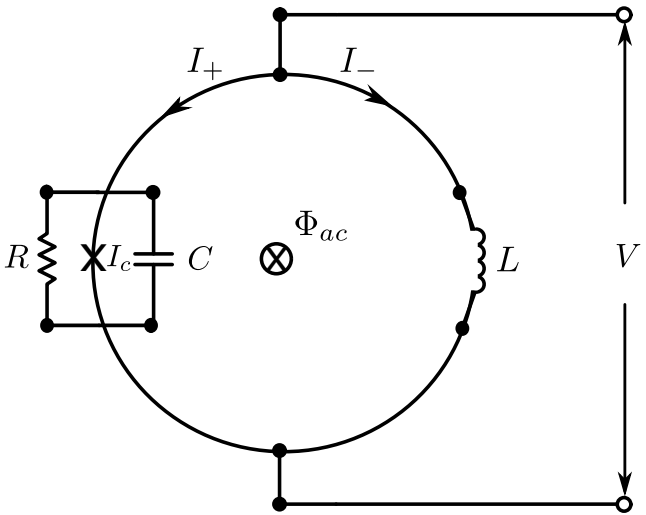

$$a_\omega = \frac{2\pi I_{\mathrm{dc}}}{f\Phi_0}\left(\frac{L}{Z_\omega}+\frac{1}{i\omega}\right)V_\omega$$

$$V_\omega = \frac{iI_\omega\omega}{C(\omega_0^2+2i\zeta\omega\omega_0-\omega^2)}$$

$$\omega_0^2 = \frac{1}{LC} - \text{resonance frequency}$$

$$\zeta = \frac{1}{2RC\omega_0} - \text{damping rate}$$

Figure 4: Circuit model of the rf SQUID-based accelerometer [3].

[3] I. Khomchenko, P. Navez, H. Ouerdane, "SQUID-based interferometric accelerometer", Appl. Phys. Lett. **121**, 152601 (2022).

Energy-Information Battery

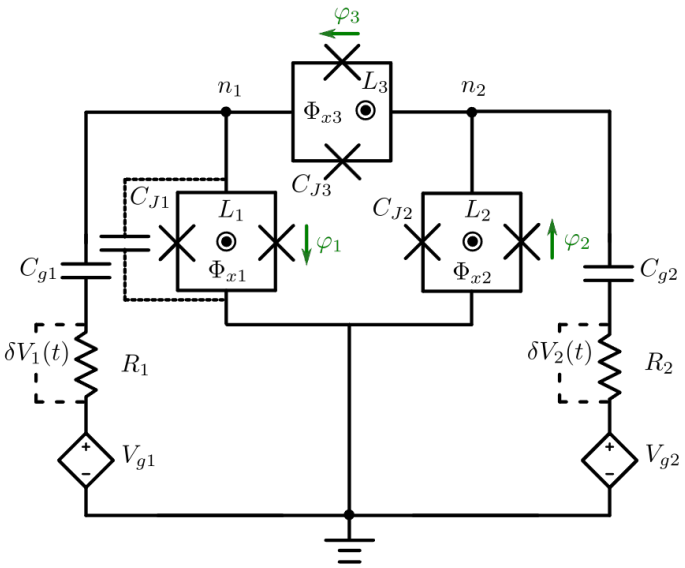

- dc SQUID can serve as a battery [4, 5];
- dc SQUID can information [6];
- Characterize this system;
- Show how energy converts into information in such a device;

Figure 5: A schematic picture of a quantum information battery.

[4] L. Bulaevskii, V. Kuzii, & A. Sobyanin, JETP Lett. 25, 290–294 (1977).
[5] E. Strambini et al. Nat. Nanotechnol. 15, 656–660 (2020).
[6] Y. Wang, Z. Wang, & C. Sun, Phys. Rev. B **72**, 172507 (2005).

Finite-time Cycle

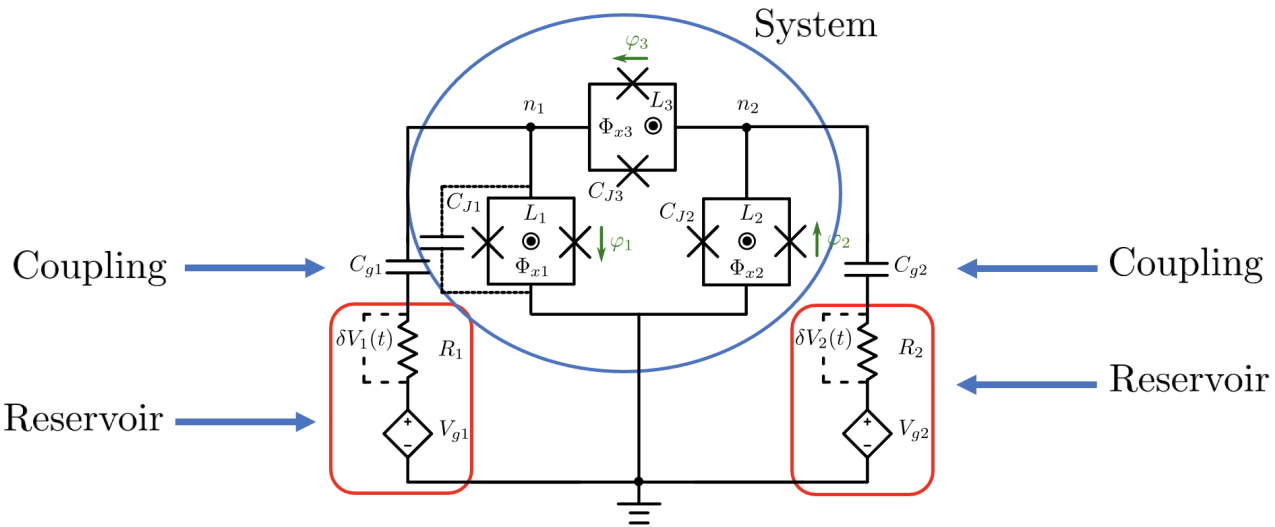

Figure 6: Circuit of a quantum information battery capacitively coupled to a bosonic thermal bath and a bath of independent spins in thermal equilibrium [6, 7].

[6] Y. Wang, Z. Wang, & C. Sun, Phys. Rev. B **72**, 172507 (2005).

[7] J. P. Pekola, & B. Karimi, Phys. Rev. X **12**, 011026 (2022).

Finite-time Cycle

Stroke I → II − disconnecting: battery (qubit 2) and charger (qubit 1) in state $\rho_{12,\mathrm{I}}$

$$E_{\mathrm{d}}(\tau_1) = E_{\mathrm{d}}(\tau_1) = \mathrm{Tr}\left\{\frac{E_C}{2}(\sigma_2^z + \sigma_1^z)\rho_{12,\mathrm{I}}(\tau_1)\right\} - \mathrm{Tr}\{\hat{H}_{\mathrm{sys}}\rho_{12,\mathrm{I}}(0)\}.$$

Stroke II → III: ergotropy extracted from the battery

$$\mathcal{E} = \mathrm{Tr}\{\hat{H}_2(\rho_{2,\mathrm{II}} - \rho_{2,\mathrm{III}})\}.$$

Stroke III → IV − connecting: during time τ_3 ($\tau_* = \tau_1 + \tau_3$)

$$E_{\mathrm{c}}(\tau_*) = \mathrm{Tr}\{\rho_{12,\mathrm{III}}(\tau_*)\hat{H}_{\mathrm{sys}}\} - \mathrm{Tr}\left\{\frac{E_C}{2}(\sigma_2^z + \sigma_1^z)\rho_{12,\mathrm{I}}(\tau_1)\right\}.$$

Stroke IV → I − thermalization during time τ_4 ($\tau_\Sigma = \tau_1 + \tau_3 + \tau_4$)

$$E_{\mathrm{th}}(\tau_\Sigma) = \mathrm{Tr}\{\hat{H}_{\mathrm{sys}}\rho_{12,\mathrm{I}}(\tau_\Sigma)\} - \mathrm{Tr}\{\hat{H}_{\mathrm{sys}}\rho_{12,\mathrm{IV}}(\tau_*)\},$$

[8] F. Barra, K. V. Hovhannisyan, & A. Imparato. New J. Phys. 24, 015003 (2022).

Finite-time Cycle

Thermalization: Lindblad Master Equation

$$\dot{\rho}_{12,\mathrm{IV}}(t) = -\frac{i}{\hbar}[\rho_{12,\mathrm{IV}}(t), \hat{H}_{\mathrm{sys}}] + \Gamma_0 \sum_{n=1}^{2} \mathcal{D}[\hat{C}_n]\hat{\rho}_{12,\mathrm{IV}}(t)$$
$$+ \sum_{\varepsilon} \Gamma_\varepsilon \mathcal{D}[\hat{L}_\varepsilon^\dagger]\hat{\rho}_{12,\mathrm{IV}}(t) + \overline{\Gamma}_\varepsilon \mathcal{D}[\hat{L}_\varepsilon]\hat{\rho}_{12,\mathrm{IV}}(t).$$

Energy conversion: Cycle's efficiency

$$\eta = \frac{\mathcal{E}}{E_{\mathrm{c}} + E_{\mathrm{d}}}.$$

Information transfer: Fidelity $\mathcal{F}$ [9]

$$\mathcal{F} = \mathrm{Tr}\sqrt{\rho_{12,\mathrm{I}}^{1/2}\rho_{12,\mathrm{IV}}(\tau_\Sigma)\rho_{12,\mathrm{I}}^{1/2}}.$$

[9] M. A. Nielsen, I. L. Chuang. Cambridge University Press (2011).

Postdoctoral Project

Why University of Malta and ASPECTS?

- Experienced team of multidisciplinary professors;
- Networking and collaborating with other research groups;
- Opportunities for innovations and entrepreneurship;
- Development of my Ph.D. research topic;
- Professional growth.

Proposed directions for postdoctoral research

Superconducting Quantum Energy-Information Battery

- Further development of a quantum information-battery;
- Collaboration with Prof. Giuliano Benenti, Dr. Luca Razioli (University of Insubria), Dr. Dario Ferarro (University of Genova), Prof. Henni Ouerdane (Skoltech);
- Assistance with students' supervision.

Proposed directions for postdoctoral research

Quantum computer-aided design (QCAD) of atomic clocks

- Develop a theory about how fault tolerant quantum computers can be used to improve the design of atomic clocks.
- Collaboration with Infleqtion and my hack's team (Paul Mandon – EFREI (France), Sabarikirishwaran Ponnambalam – Qubrid (USA));
- Assistance with students' supervision.

Quantum computer-aided design of atomic clocks

- Fault tolerant quantum computing logical: error-corrected fidelity $\mathcal{F} \geq 99\%$ (suppressed logical errors).
- Averaged gate fidelity

$$\mathcal{F} = \frac{2 + e^{-\frac{\theta^2}{2N}}}{3},$$

where θ is the pulse area and N is the accuracy [10].

- Account for the quantum projection noise (QPN)

$$\sigma_{\mathrm{QPN}}(\tau) = \frac{1}{2\pi\nu C T}\sqrt{\frac{T + T_{\mathrm{d}}}{N_{\mathrm{a}}\tau}},$$

where ν is the clock transition frequency, C is the contrast, T is the coherent interrogation time, T_{d} is the dead time, τ is the averaging time, and N_{a} is the number of atoms being interrogated.

[10] J. Xuereb, et al. Phys. Rev. Lett. **131**, 160204 (2023).

[11] X. Zheng, J. Dolde and S. Kolkowitz. Phys. Rev. X **14**, 011006 (2024).

Thank you for your attention!

[1] Dettori, R., Melis, C., Rurali, R. & Colombo, L.
Thermal rectification in silicon by a graded distribution of defects.
Journal of Applied Physics **119**, 215102 (2016).

[2] Khomchenko, I., Ouerdane, H. & Benenti, G.
Voltage-amplified heat rectification in sis junctions.
Physical Review B **106**, 245413 (2022).

[3] Khomchenko, I., Navez, P. & Ouerdane, H.
Squid-based interferometric accelerometer.
Applied Physics Letters **121** (2022).

[4] Bulaevskii, L., Kuzii, V. & Sobyanin, A.
Superconducting system with weak coupling to the current in the ground state.
JETP lett **25**, 290–294 (1977).

[5] Strambini, E. *et al.*
A josephson phase battery.
Nature Nanotechnology **15**, 656–660 (2020).

[6] Wang, Y., Wang, Z. & Sun, C.
Quantum storage and information transfer with superconducting qubits.
Physical Review B **72**, 172507 (2005).

[7] Pekola, J. P. & Karimi, B.
Ultrasensitive calorimetric detection of single photons from qubit decay.
Physical Review X **12**, 011026 (2022).

[8] Barra, F., Hovhannisyan, K. V. & Imparato, A.
Quantum batteries at the verge of a phase transition.
New Journal of Physics **24**, 015003 (2022).

[9] Nielsen, M. A. & Chuang, I. L.
Quantum computation and quantum information (Cambridge university press, 2010).

[10] Xuereb, J., Erker, P., Meier, F., Mitchison, M. T. & Huber, M.
Impact of imperfect timekeeping on quantum control.
Physical Review Letters **131**, 160204 (2023).

[11] Zheng, X., Dolde, J. & Kolkowitz, S.
Reducing the instability of an optical lattice clock using multiple atomic ensembles.
Physical Review X **14**, 011006 (2024).

[12] Guttman, G. D., Nathanson, B., Ben-Jacob, E. & Bergman, D. J.
Phase-dependent thermal transport in josephson junctions.
Physical Review B **55**, 3849 (1997).

[13] Larkin, A. & Ovchinnikov, Y. N.
Tunnel effect between superconductors in an alternating field.
Sov. Phys. JETP **24**, 1035–1040 (1967).

[14] Marchegiani, G., Braggio, A. & Giazotto, F.
Phase-tunable thermoelectricity in a Josephson junction.
Physical Review Research **2**, 043091 (2020).

[15] Storey, P. & Cohen-Tannoudji, C.
The feynman path integral approach to atomic interferometry. a tutorial.
Journal de Physique II **4**, 1999–2027 (1994).

[16] Navez, P. *et al.*
Matter-wave interferometers using taap rings.
New Journal of Physics **18**, 075014 (2016).

[17] Hofer, P. P. *et al.*
Markovian master equations for quantum thermal machines: local versus global approach.
New Journal of Physics **19**, 123037 (2017).

[18] Costa, A., Beims, M. & Strunz, W.
System-environment correlations for dephasing two-qubit states coupled to thermal baths.
Physical Review A **93**, 052316 (2016).

[19] Tornow, S., Gehrke, W. & Helmbrecht, U.
Non-equilibrium dynamics of a dissipative two-site hubbard model simulated on ibm quantum computers.
Journal of Physics A: Mathematical and Theoretical **55**, 245302 (2022).

[20] Andolina, G. M. *et al.*
Charger-mediated energy transfer in exactly solvable models for quantum batteries.
Physical Review B **98**, 205423 (2018).

[21] Ferraro, D., Campisi, M., Andolina, G. M., Pellegrini, V. & Polini, M.
High-power collective charging of a solid-state quantum battery.
Physical review letters **120**, 117702 (2018).

[22] Crescente, A., Ferraro, D., Carrega, M. & Sassetti, M.
Enhancing coherent energy transfer between quantum devices via a mediator.
Physical Review Research **4**, 033216 (2022).

[23] Campaioli, F., Gherardini, S., Quach, J. Q., Polini, M. & Andolina, G. M.
Colloquium: Quantum batteries.
arXiv preprint arXiv:2308.02277 (2023).

[24] Hoang, D. T. *et al.*
Variational quantum algorithm for ergotropy estimation in quantum many-body batteries.
Physical Review Research **6**, 013038 (2024).

[25] Blais, A., Grimsmo, A. L., Girvin, S. M. & Wallraff, A.
Circuit quantum electrodynamics.
Reviews of Modern Physics **93**, 025005 (2021).

[26] Brask, J. B., Haack, G., Brunner, N. & Huber, M.
Autonomous quantum thermal machine for generating steady-state entanglement.
New Journal of Physics **17**, 113029 (2015).

[27] Cattaneo, M., Giorgi, G. L., Maniscalco, S. & Zambrini, R.
Local versus global master equation with common and separate baths: superiority of the global approach in partial secular approximation.
New Journal of Physics **21**, 113045 (2019).

Appendix

Adiabatic Regime

Let us consider a case of a non-zero voltage, i.e., $V \neq 0$.

The contribution from $\dot{Q}_j \neq 0$ [12]. So, there are all three terms $\dot{Q}_{\rm qp}$, $\dot{Q}_{\rm int}$, and $\dot{Q}_{\rm j}$.

Then, we take $V_s(t) = V_0 \ \sin(\Omega t)$.

When $eV_0 \ll \Delta$ and $\hbar\Omega \ll \Delta$, the heat current is [12, 13]

$$\dot{Q}_{\rm fw,bw} = \pm\dot{Q}_{\rm qp;fw,bw} + \dot{Q}_{j;\rm fw,bw} \ \sin\varphi \pm \dot{Q}_{\rm int;fw,bw} \ \cos\varphi.$$

[12] G. D. Gutman et al., Phys. Rev. B 55, 3849 (1997).

[13] A. Larkin and Y. N. Ovchinnikov, Sov. Phys. JETP 24, 1035–1040 (1967).

Beyond the Adiabatic Regime

Voltage: $V(t) = V_s(t) + V_r(t)$, with the slowly-varying potential, $V_s(t)$, and the rapidly-varying potential, $V_r(t)$.

The rapidly varying potential $V_{\mathrm{r}}(t)$:

$$V_{\mathrm{r}}(t) = \int_{-\infty}^{\infty} V(\omega) e^{-i\omega t} \frac{d\omega}{2\pi}.$$

For $V_{\mathrm{r}} = V_0 \cos(\omega_0 t)$, $V(\omega) = V_0 \pi[\delta(\omega - \omega_0) + \delta(\omega + \omega_0)]$.

Heat currents in the Non-Adiabatic Regime

$$\dot{Q}_i(t) = \dot{Q}_i(\omega_0 t) + \dot{Q}_i(-\omega_0 t),$$

with

$$\begin{aligned}
&\dot{Q}_i(\omega_0 t) = \\
&\frac{eV_{\mathrm{r0}}}{\hbar\omega_0}\left[\dot{Q}_{\mathrm{int};i}(V_{\mathrm{s0}} + \hbar\omega_0/e) - \dot{Q}_{\mathrm{int};i}(V_{\mathrm{s0}})\right]\cos(\varphi_{\mathrm{s}}(t) - \omega_0 t) \\
&+ \frac{eV_{\mathrm{r0}}}{\hbar\omega_0}\left[\dot{Q}_{\mathrm{j};i}(V_{\mathrm{s0}} + \hbar\omega_0/e) - \dot{Q}_{\mathrm{j};i}(V_{\mathrm{s0}})\right]\sin(\varphi_{\mathrm{s}}(t) - \omega_0 t) \\
&+ \frac{eV_{\mathrm{r0}}}{\hbar\omega_0}\left[\dot{Q}_{\mathrm{qp};i}(V_{\mathrm{s0}} + \hbar\omega_0/e) - \dot{Q}_{\mathrm{qp};i}(V_{\mathrm{s0}})\right]\cos(\omega_0 t) \\
&+ \frac{eV_{\mathrm{r0}}}{\hbar\omega_0}\left[\dot{Q}_{\mathrm{qpr};i}(V_{\mathrm{s0}} + \hbar\omega_0/e) - \dot{Q}_{\mathrm{qpr};i}(V_{\mathrm{s0}})\right]\sin(-\omega_0 t),
\end{aligned}$$

where $\varphi_{\mathrm{s}}(t) = 2e/\hbar \int^t V_{\mathrm{s}}(t')\mathrm{d}t'$ is a slow-varying phase.

Heat currents in the Non-Adiabatic Regime

$\dot{Q}_{\mathrm{qpr}}$ is the reactive part of the quasiparticle heat current.

$\dot{Q}_{\mathrm{qpr}}$ is the Kramers-Kronig transform of the quasiparticle heat current $\dot{Q}_{\mathrm{qp}}$.

The last formula is only valid for $eV_0 \ll \hbar\omega_0$.

Microscopic Expressions of the Heat Currents

$$Q_{\mathrm{qp};i} = \frac{G}{e^2}\int_{-\infty}^{\infty} E_k \ \mathrm{Im}[N_k(E_k)]\mathrm{Im}[N_m(E_m)][f_k(E_k) - f_m(E_m)] \ \mathrm{d}E,$$

$$\begin{aligned} Q_{\mathrm{j};i} \quad &= \quad \frac{G}{2e^2}\int_{-\infty}^{\infty} E_k \Bigg\{ \mathrm{Im}[F_k(-jE_k)]\mathrm{Re}[F_m(jE_m)]\tanh\left(\frac{E_k}{2k_{\mathrm{B}}T_k}\right) \\ &+ \quad \mathrm{Im}[F_m(jE_m)]\mathrm{Re}[F_k(-jE_k)]\tanh\left(\frac{E_m}{2k_{\mathrm{B}}T_m}\right)\Bigg\} \ \mathrm{d}E, \end{aligned}$$

Microscopic Expressions of the Heat Currents

$$Q_{\mathrm{int};i} = \frac{G}{e^2}\int_{-\infty}^{\infty} E_k \ \mathrm{Im}[F_k(-jE_k)]\mathrm{Im}[F_m(jE_m)][f_k(E_k) - f_m(E_m)] \ \mathrm{d}E,$$

$$\begin{aligned} Q_{\mathrm{qpr};i} &= \frac{G}{2e^2}\int_{-\infty}^{\infty} E_k \Bigg\{ \mathrm{Im}[N_k(E_k)]\mathrm{Re}[N_m(E_m)]\tanh\left(\frac{E_k}{2k_{\mathrm{B}}T_k}\right) \\ &+ \mathrm{Im}[N_m(E_m)]\mathrm{Re}[N_k(E_k)]\tanh\left(\frac{E_m}{2k_{\mathrm{B}}T_m}\right)\Bigg\} \ \mathrm{d}E, \end{aligned}$$

where Re[...] and Im[...] denote the real and imaginary parts, $j^2 = -1$, $i \equiv$ fw (bw), $m =$ R and $k =$ L for the forward flux and vice versa for the backward flux, and $E_k = E - \mu_k$ [14].

[14] G. Marchegiani, A. Braggio, and F. Giazotto, Phys. Rev. Res. 2, 043091 (2020).

Special Functions

According to the BCS model, the quasiparticle densities of states are given by

$$N_k(E) = -\frac{E + j\Gamma_k}{\sqrt{(E + j\Gamma_k)^2 - \Delta_k^2}}$$

The anomalous Green functions are

$$F_k(E) = \frac{j\Delta_k}{\sqrt{\Delta_k^2 - (E + j\Gamma_k)^2}},$$

where $\Gamma_k = 10^{-4}\Delta_k(0)$ are the Dynes parameters, $G = 10^{-3}\ \Omega^{-1}$ is the normal state electrical conductance of the junction.

Special Functions

According to the BCS model, the quasiparticle densities of states are given by

$$N_k(E) = -\frac{E + j\Gamma_k}{\sqrt{(E + j\Gamma_k)^2 - \Delta_k^2}}$$

The anomalous Green functions are

$$F_k(E) = \frac{j\Delta_k}{\sqrt{\Delta_k^2 - (E + j\Gamma_k)^2}},$$

where $\Gamma_k = 10^{-4}\Delta_k(0)$ are the Dynes parameters, $G = 10^{-3}\ \Omega^{-1}$ is the normal state electrical conductance of the junction.

Phase Calculation

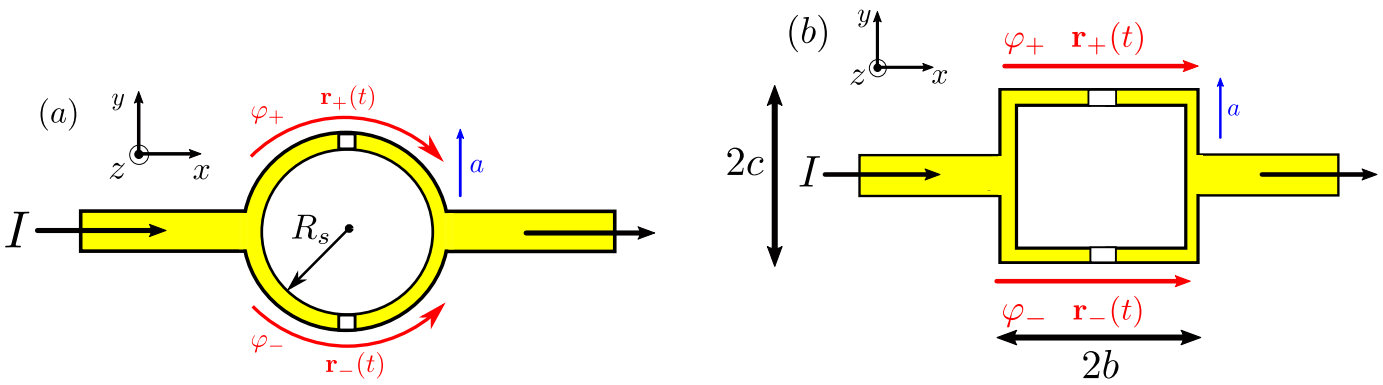

Figure 7: Scheme of a SQUID designed in two geometries: (a) ring and (b) rectangular.

Total current induced by the Cooper pairs motion is

$$I = 2I_c \cos\left(\frac{\delta\varphi}{2}\right),$$

where $\Delta\varphi = 0$, and $\delta\varphi = 2\pi\Phi_B/\Phi_0$ is the phase shift caused by an external magnetic field, $\mathbf{B}$.

Phase Calculation

Phase shift occurs due to acceleration, a, is the net phase given by the difference of the phases accumulated in each arm $\pm$ [15, 16]

$$\delta\varphi \quad = \quad \varphi_+ - \varphi_- \qquad \text{with} \quad \varphi_\pm = \int_0^{t_\pm} \frac{m\dot{\mathbf{r}}_\pm^2(t)}{2\hbar} \mathrm{d}t,$$

where $\dot{\mathbf{r}}_\pm$ is the superconducting fraction's center of mass velocity in each arm of the SQUID, and $t_\pm$ are the traveling times along the trajectories $\mathbf{r}_\pm(t)$ from the beginning to the end of each arm. [15] P.

Storey and C. Cohen-Tannoudji, Journal de Physique II. 4, 1999 (1994).

[16] P. Navez et al., New J. Phys. 18, 075014 (2016).

Phase Calculation

For the ring geometry with the radius R_s:
$\mathbf{r}_\pm(t) = (R_\mathrm{s}\cos(\Omega t), \pm R_\mathrm{s}\sin(\Omega t) + at^2/2, 0)$, where $\Omega = v/R_\mathrm{s}$ is the effective angular velocity, and v is the drift velocity.

Total phase accumulated along the loop as

$$\delta\varphi = -2\frac{m}{\hbar}\int_0^{\pi/\Omega} R_\mathrm{s} a\Omega t\cos(\Omega t)\mathrm{d}t = f\frac{a}{I}$$

where $f = 4mR_\mathrm{s}^2 I/(\hbar v)$ is a form factor associated to the SQUID geometry.

Coulomb Hamiltonian

The Coulomb Hamiltonian $\hat{H}_c$ is

$$\hat{H}_c = E_{C1}(\hat{N}_1 - N_{g1})^2 + E_{C2}(\hat{N}_2 - N_{g2})^2 + 4E_{C3}(\hat{N}_1 - N_{g1})(\hat{N}_2 - N_{g2}),$$

where N_i is the number of the excess Cooper pairs in the ith Cooper pair box, and $N_{gi} = C_{gi}V_{gi}/2e$ is dimensionless gate charge.

Here, $E_{C1} = 2e^2 C_{\Sigma 2}/(C_{\Sigma 1}C_{\Sigma 2} - C_{J3}^2)$, $E_{C2} = 2e^2 C_{\Sigma 1}/(C_{\Sigma 1}C_{\Sigma 2} - C_{J3}^2)$, and $E_{C3} = e^2 C_{\Sigma 2}/2(C_{\Sigma 1}C_{\Sigma 2} - C_{J3}^2)$ with $C_{\Sigma i} = C_{Ji} + C_3 + C_{gi}$ [6].

[6] Y. Wang, Z. Wang, & C. Sun, Phys. Rev. B 72, 172507 (2005).

Hamiltonian in two-spin notations

It is convenient to rewrite the Hamiltonian as the Hamiltonian of a two-level system

$$\hat{H} = \sum_{i=1}^{2} \Omega_i \sigma_i^z + E_{C3} \sigma_1^z \sigma_2^z + \hat{H}_{\text{bath}-\text{sys}} + \hat{H}_{\text{bath}}$$
$$-E_{J3} \cos\left(\frac{\pi\Phi_{x3}}{\Phi_0} + \frac{\varphi_{tot,3}}{2}\right)\left\{1 - \frac{5}{2}\left(\frac{\pi L_3 I_{c,3}}{\Phi_0}\right)^2 \sin^2\left(\frac{\pi\Phi_{x3}}{\Phi_0} + \frac{\varphi_{tot,3}}{2}\right)\right\}(\sigma_1^x\sigma_2^x - \sigma_1^y\sigma_2^y)$$
$$-\sum_{i=1}^{2} E_{Ji} \cos\left(\frac{\pi\Phi_{xi}}{\Phi_0} + \frac{\varphi_{tot,i}}{2}\right)\left\{1 - \frac{5}{2}\left(\frac{\pi L_i I_{c,i}}{\Phi_0}\right)^2 \sin^2\left(\frac{\pi\Phi_{xi}}{\Phi_0} + \frac{\varphi_{tot,i}}{2}\right)\right\}\sigma_i^x,$$

where $\Omega_i = E_{ci}(N_{gi} - 0.5) + 2E_{C3}(N_{gj} - 0.5)(i \neq j)$ and $\sigma^{j=x,y,z}$ are the Pauli matrices.

Environment: Thermalization

The environment is a bath of independent harmonic oscillators of the system in thermal equilibrium [17, 18].

$$\hat{H}_{\text{bath}-\text{sys;th}} = \hbar(\sigma_z \otimes \mathbb{I} + \mathbb{I} \otimes \sigma_z) \otimes \sum_{\alpha=1}^{d} \gamma_\alpha (\hat{b}_\alpha^\dagger \hat{a} + \hat{b}_\alpha \hat{a}^\dagger),$$

$$\hat{H}_{\text{bath;th}} = \sum_{\alpha=1}^{d} \hbar\omega_\alpha \hat{b}_\alpha^\dagger \hat{b}_\alpha,$$

where σ_z is the system spin, ω_α are the frequencies of the environment mode, γ_α is the coupling coefficient for the αth mode, $\hat{a}$ ($\hat{b}_\alpha$) denote annihilation operators of the system (bath), and d is the number of bath modes.

[17] P.P. Hofer, et al. New J. Phys. 19, 123037 (2017).

[18] A. Costa, M. Beims, & W. Strunz, Phys. Rev. A 93, 052316 (2016).

Environment: Decoherence

The environment is a bath of independent two-level systems (spins) in thermal equilibrium [19].

$$\hat{H}^{ZZ}_{\text{bath-sys,dc}} = \hbar \sum_{\alpha=1}^{d} g_\alpha([\sigma_z \otimes \mathbb{I} + \mathbb{I} \otimes \sigma_z] \otimes \sigma_{z,\alpha}),$$

$$\hat{H}^{ZZ}_{\text{bath,dc}} = -\sum_{\alpha=1}^{d} \hbar\omega_\alpha \sigma_{x,\alpha},$$

where $\sigma_z(\sigma_{z,\alpha})$ is the system spin (bath spin), ω_α are the frequencies of the environment mode, g_α is the coupling coefficient for the αth mode and d is the number of bath modes.

[19] S. Tornow, W. Gehrke, & U. Helmbrecht, J. Phys. A Math. Theor. 55, 245302 (2022).

Energy

The energy deposited inside one qubit at time t starting from some initial state $\rho(0)$ is measured with respect to the internal Hamiltonian, $\hat{H}_i$, [20, 21, 22]

$$E_i(t) \equiv \mathrm{Tr}\{\rho(t)\hat{H}_i\} - \mathrm{Tr}\{\rho(0)\hat{H}_i\},$$

where $i = 1, 2$; ρ is the density matrix of the system i and $\mathrm{Tr}\{...\}$ is the conventional trace operation. $\hat{H}_i$ is given by

$$\hat{H}_i = \Omega_i \sigma_i^z - E_{Ji} \cos\left(\frac{\pi\Phi_{xi}}{\Phi_0} + \frac{\varphi_{\mathrm{tot,i}}}{2}\right)$$
$$\left\{1 - \frac{5}{2}\left(\frac{\pi L_i I_{c,i}}{\Phi_0}\right)^2 \sin^2\left(\frac{\pi\Phi_{xi}}{\Phi_0} + \frac{\varphi_{\mathrm{tot,i}}}{2}\right)\right\}\sigma_i^x,$$

[20] G. M. Andolina, et al., Phys. Rev. B 98, 205423 (2018).
[21] D. Ferraro, M. Campisi, G. M. Andolina, V. Pellegrini, & M. Polini, Phys. Rev. Lett. 120, 117702 (2018).
[22] A. Crescente, D. Ferraro, M. Carrega, & M. Sassetti, Phys. Rev. Res. 4, 033216 (2022).

Energy

The energy extracted from the system E_{out} is simply related to the energy deposited E_{in} by the following relation $E_{\text{in}} = -E_{\text{out}} = E_i$ [23]. The energy associated with interactions is [20, 21, 22]

$$E_{\text{int}}(t) \equiv \text{Tr}\{\rho(t)\hat{H}_{\text{int}}\} - \text{Tr}\{\rho(0)\hat{H}_{\text{int}}\},$$

where $\hat{H}_{\text{int}}$ is given by

$$\hat{H}_{\text{int}} = E_{C3}\sigma_1^z\sigma_2^z - E_{J3}\cos\left(\frac{\pi\Phi_{x3}}{\Phi_0} + \frac{\varphi_{\text{tot},3}}{2}\right)$$
$$\left\{1 - \frac{5}{2}\left(\frac{\pi L_3 I_{c,3}}{\Phi_0}\right)^2 \sin^2\left(\frac{\pi\Phi_{x3}}{\Phi_0} + \frac{\varphi_{\text{tot},3}}{2}\right)\right\}(\sigma_1^x\sigma_2^x - \sigma_1^y\sigma_2^y)$$

Battery: Operation

Next, we consider the total Hamiltonian

$$\hat{H}_{\text{tot}} = \hat{H}_1 + \hat{H}_2 + \hat{H}_{\text{int}} + \hat{H}_{\text{bath-sys,th}} + \hat{H}_{\text{bath,th}} + \hat{H}_{\text{bath-sys,dc}} + \hat{H}_{\text{bath,dc}},$$

where we call qubit 1 a charger and qubit 2 a battery, which are assumed to be strongly coupled with each other.

In this case, we can perform a cycle, which has four strokes, treating this system as isolated for the three strokes.

For convenience, we consider the system's Hamiltonian [8]

$$\hat{H}_{\text{sys}} = \hat{H}_1 + \hat{H}_2 + \hat{H}_{\text{int}}.$$

[8] F. Barra, K. V. Hovhannisyan, & A. Imparato. New J. Phys. 24, 015003 (2022).

Physical parameters

As we deal with a real system, the density matrix at the beginning of the cycle was chosen as

$$\rho_{12,\mathrm{I}} = \frac{e^{-\beta \hat{H}_{\mathrm{sys}}}}{Z_{\mathrm{sys}}}, \tag{1}$$

where $\beta = 1/k_B T$, T is the temperature of the whole system, with $Z_{\mathrm{sys}} = \mathrm{Tr}\{e^{-\beta \hat{H}_{\mathrm{sys}}}\}$.

Finite-time Cycle

Stroke I → II: the battery and the charger are in the state $\rho_{12,\mathrm{I}}$. During this stage, qubit 2 is disconnected from qubit 1 during time $\tau_1 = 300$ ns, which results in the energy cost

$$E_{\mathrm{d}}(\tau_1) = \mathrm{Tr}\{\rho_{12,\mathrm{I}}(\tau_1)\hat{H}_{\mathrm{sys}}\} - \mathrm{Tr}\{\rho_{12,\mathrm{I}}(0)\hat{H}_{\mathrm{sys}}\}.$$

The evolution of the density matrix $\rho_{12,\mathrm{I}}(t)$ satisfies the von Neumann equation

$$\dot{\rho}_{12,\mathrm{I}}(t) = -\frac{i}{\hbar}[\hat{H}_{\mathrm{sys}}, \rho_{12,\mathrm{I}}(t)].$$

The density matrix $\rho_{12,\mathrm{I}}(t)$ evolves in $t \in [0, \tau_1]$ in this stroke. During this stroke, we switch on the magnetic flux, $\Phi(s) = (1-s)\Phi_{\mathrm{i}} + s\Phi_{\mathrm{f}}$, with $s = t/\tau_1$.

Finite-time Cycle

Stroke II $\rightarrow$ III: at the beginning of stage II, qubit 2 is in the state

$$\rho_{2,\mathrm{II}}(\tau_1) = \mathrm{Tr}\{\rho_{12,\mathrm{I}}(\tau_1)\}.$$

We can extract ergotropy $\mathcal{E}$ from qubit 2, changing $\rho_{2,\mathrm{II}}$ to $\rho_{2,\mathrm{III}}$

$$\rho_{2,\mathrm{III}}(t) = U_{\mathcal{E}}(t)\rho_{2,\mathrm{II}}(t)U_{\mathcal{E}}^{\dagger}(t).$$

This state becomes the passive state of qubit 2, and $U_{\mathcal{E}}$ is a unitary operator that extracts the ergotropy $\mathcal{E}$ from this qubit.

The evolution of the density matrix $\rho_{2,\mathrm{II}}(t)$ satisfies the von Neumann equation

$$\dot{\rho}_{2,\mathrm{II}}(t) = -\frac{i}{\hbar}[\hat{H}_2, \rho_{2,\mathrm{II}}].$$

The density matrix $\rho_{2,\mathrm{II}}(t)$ evolves in $t \in [\tau_1, \tau_1 + \tau_2]$ in this stroke, where the magnetic flux, $\Phi = \Phi_{\mathrm{f}}$.

Finite-time Cycle

We assume that ergotropy extraction takes $\tau_2 \approx 0.4\tau_1 = 120$ ns [24].

The unitary operator $U_{\mathcal{E}}$ is determined by the spectral decomposition of $\rho_{2,\mathrm{II}}$ and $\hat{H}_2$

$$\begin{aligned} \rho_{2,\mathrm{II}}(t) &= \rho_-(t)\,|\rho_-(t)\rangle\,\langle\rho_-(t)| + \rho_+(t)\,|\rho_+(t)\rangle\,\langle\rho_+(t)| \\ H_2 &= e_+\,|e_+\rangle\,\langle e_+| + e_-\,|e_-\rangle\,\langle e_-|\,, \end{aligned}$$

where $\rho_\pm$ denotes the larger (smaller) eigenvalue of ρ_2 with the corresponding $|\rho_\pm\rangle$ eigenvectors, while $e_\pm$ and $|e_\pm\rangle$ are the eigenvalues and eigenvectors of $\hat{H}_2$.

[24] D. T. Hoang, et al. Phys. Rev. Res. 6, 013038 (2024).

Finite-time Cycle

The unitary operator $U_{\mathcal{E}}$ is [8]

$$U_{\mathcal{E}}(t) = |e_-\rangle \langle \rho_+(t)| + |e_+\rangle \langle \rho_-(t)| .$$

Following this, the II $\rightarrow$ III transition results in a new state

$$\rho_{12,\mathrm{III}}(t) = \mathcal{U}_{\mathcal{E}}(t)\rho_{12,\mathrm{II}}(t)\mathcal{U}_{\mathcal{E}}^{\dagger}(t),$$

where $\rho_{12,\mathrm{II}}(\tau_1) = \rho_{12,\mathrm{I}}(\tau_1)$, with $\mathcal{U}_{\mathcal{E}}(t) = U_{\mathcal{E}}(t) \otimes \mathbb{I}_1$.

The ergotropy extracted from qubit 2 is

$$\mathcal{E}(\tau_1 + \tau_2) = \mathrm{Tr}\{\hat{H}_2(\rho_{2,\mathrm{II}}(\tau_1) - \rho_{2,\mathrm{III}}(\tau_1 + \tau_2))\},$$

where $\rho_{12,\mathrm{II}}(\tau_1 + \tau_2) = \rho_{12,\mathrm{III}}(\tau_1 + \tau_2)$.

[8] F. Barra, K. V. Hovhannisyan, & A. Imparato. New J. Phys. 24, 015003 (2022).

Finite-time Cycle

Stroke III → IV: we reconnect qubit 1 and qubit 2 during time, $\tau_3 = 300$ ns, with the energy cost

$$E_{\rm c}(\tau_*) = {\rm Tr}\{\rho_{12,{\rm III}}(\tau_*)\hat{H}_{\rm sys}\} - {\rm Tr}\{\rho_{12,{\rm III}}(\tau_1+\tau_2)\hat{H}_{\rm sys}\},$$

where $\tau_* = \tau_1 + \tau_2 + \tau_3$.

The evolution of the density matrix $\rho_{12,{\rm III}}(t)$ satisfies the von Neumann equation

$$\dot{\rho}_{12,{\rm III}}(t) = -\frac{i}{\hbar}[\hat{H}_{\rm sys}, \rho_{12,{\rm III}}],$$

where $\rho_{12,{\rm III}}(\tau_1+\tau_2+\tau_3) = \rho_{12,{\rm IV}}(\tau_1+\tau_2+\tau_3)$.

The density matrix $\rho_{12,{\rm III}}(t)$ evolves in $t \in [\tau_1+\tau_2, \tau_*]$ in this stroke. During this stroke, we switch on the magnetic flux, $\Phi(s) = s\Phi_{\rm i} + (1-s)\Phi_{\rm f}$, with $s = t/\tau_3$.

Finite-time Cycle

To close the cycle, we perform the **Stroke IV** $\rightarrow$ **I**, by connecting the full system to a reservoir during the time τ_4.

In this case, the heat delivered to qubit 1 and 2 is

$$E_{\mathrm{th}}(\tau_\Sigma) = \mathrm{Tr}\{\hat{H}_{\mathrm{sys}}\rho_{12,\mathrm{I}}(\tau_\Sigma)\} - \mathrm{Tr}\{\hat{H}_{\mathrm{sys}}\rho_{12,\mathrm{IV}}(\tau_*)\},$$

which is not the energy cost to run the cycle.

The evolution of the density matrix $\rho_{12,\mathrm{IV}}(t)$ satisfies the Lindblad equation [25]

$$\dot{\rho}_{12,\mathrm{IV}}(t) = -\frac{i}{\hbar}[\hat{H}_{\mathrm{sys}}, \rho_{12,\mathrm{IV}}(t)] + \sum_{d=1}^{N} \Gamma_{0d}\mathcal{D}[\hat{C}_d]\hat{\rho}_{12,\mathrm{IV}}(t)$$

$$+ \sum_{d=1}^{N} 2\Gamma_{d,\varphi}\mathcal{D}[\hat{C}_d{}^\dagger \hat{C}_d]\hat{\rho}_{12,\mathrm{IV}}(t) + \Gamma_d\mathcal{D}[\hat{L}_d^\dagger]\hat{\rho}_{12,\mathrm{IV}}(t) + \overline{\Gamma}_d\mathcal{D}[\hat{L}_d]\hat{\rho}_{12,\mathrm{IV}}(t).$$

[25] A. Blais, A. L. Grimsmo, S. M. Girvin, & A. Wallraff, Rev. Mod. Phys. 93, 025005 (2021).

Environment: Parameters

The decay rate Γ_{0d} is given by [7]

$$\Gamma_{0d} = \left(\frac{C_g}{C_\Sigma}\right)^2 \frac{R}{Z_{\text{sys}}}\Omega,$$

$Z_{\text{sys}} = \sqrt{\frac{L_{\text{sys}}}{C_{\text{sys}}}}$ is the total impedance of the circuit.

$$\Omega = \frac{E_J}{\hbar}\cos\left(\frac{\pi\Phi_x}{\Phi_0} + \varphi_0\right)\left\{1 - \frac{5}{2}\left(\frac{\pi L I_c}{\Phi_0}\right)^2 \sin^2\left(\frac{\pi\Phi_x}{\Phi_0} + \varphi_0\right)\right\}$$

is qubit frequency and $C_\Sigma = C_g + C_{\text{sys}}$.

[7] J. P. Pekola, & B. Karimi, Phys. Rev. X 12, 011026 (2022).

Lindblad Master Equation

$$\dot{\rho}_{12,\mathrm{IV}}(t) = -\frac{i}{\hbar}[\hat{H}_{\mathrm{sys}}, \rho_{12,\mathrm{IV}}(t)] + \sum_{d=1}^{N} \Gamma_{0d}\mathcal{D}[\hat{C}_d]\hat{\rho}_{12,\mathrm{IV}}(t)$$

$$+ \sum_{d=1}^{N} 2\Gamma_{d,\varphi}\mathcal{D}[\hat{C}_d{}^{\dagger}\hat{C}_d]\hat{\rho}_{12,\mathrm{IV}}(t) + \Gamma_d\mathcal{D}[\hat{L}_d^{\dagger}]\hat{\rho}_{12,\mathrm{IV}}(t) + \overline{\Gamma}_d\mathcal{D}[\hat{L}_d]\hat{\rho}_{12,\mathrm{IV}}(t).$$

Γ_{0d} is the relaxation rate of the system that is related to the qubit-environment coupling strength evaluated at the qubit frequency.

$\Gamma_{d,\varphi}$ is the pure dephasing rate.

The rates Γ_0 and Γ_φ are related to the characteristic T_1 relaxation time and T_2 coherence time of the qubit

$$T_1 = \frac{1}{\Gamma_0}; \qquad T_2 = \left(\frac{\Gamma_0}{2} + \Gamma_\varphi\right)^{-1}.$$

Lindblad Master Equation

$$\dot{\rho}_{12,\mathrm{IV}}(t) = -\frac{i}{\hbar}[\hat{H}_{\mathrm{sys}}, \rho_{12,\mathrm{IV}}(t)] + \sum_{d=1}^{N} \Gamma_{0d}\mathcal{D}[\hat{C}_d]\hat{\rho}_{12,\mathrm{IV}}(t)$$

$$+ \sum_{d=1}^{N} 2\Gamma_{d,\varphi}\mathcal{D}[\hat{C}_d{}^{\dagger}\hat{C}_d]\hat{\rho}_{12,\mathrm{IV}}(t) + \Gamma_d\mathcal{D}[\hat{L}_d^{\dagger}]\hat{\rho}_{12,\mathrm{IV}}(t) + \overline{\Gamma}_d\mathcal{D}[\hat{L}_d]\hat{\rho}_{12,\mathrm{IV}}(t).$$

Here, $\mathcal{D}[\hat{C}_d]\hat{\rho}_{12,\mathrm{IV}}(t) = \hat{C}_d\hat{\rho}_{12,\mathrm{IV}}(t)\hat{C}_d^{\dagger} - 1/2\{\hat{C}_d^{\dagger}\hat{C}_d, \hat{\rho}_{12,\mathrm{IV}}(t)\}$.

Here, $\hat{L}_d$ are the jump operators and $\Gamma_d, \overline{\Gamma}_d$ are the corresponding rates.

Let us consider bosonic bath, for which the rates are [17, 26]

$$\Gamma_d = \kappa(\varepsilon)n_B(\varepsilon) \qquad \overline{\Gamma}_d = \kappa(\varepsilon)[n_B(\varepsilon) + 1];$$

[17] P.P. Hofer, et al. New J. Phys. 19, 123037 (2017).

[26] J.B. Brask, G. Haack, N. Brunner, & M. Huber, New J. Phys. 17, 113029 (2015).

Lindblad Master Equation

$$\dot{\rho}_{12,\mathrm{IV}}(t) = -\frac{i}{\hbar}[\hat{H}_{\mathrm{sys}}, \rho_{12,\mathrm{IV}}(t)] + \sum_{d=1}^{N} \Gamma_{0d}\mathcal{D}[\hat{C}_d]\hat{\rho}_{12,\mathrm{IV}}(t)$$

$$+ \sum_{d=1}^{N} 2\Gamma_{d,\varphi}\mathcal{D}[\hat{C}_d{}^{\dagger}\hat{C}_d]\hat{\rho}_{12,\mathrm{IV}}(t) + \Gamma_d\mathcal{D}[\hat{L}_d^{\dagger}]\hat{\rho}_{12,\mathrm{IV}}(t) + \overline{\Gamma}_d\mathcal{D}[\hat{L}_d]\hat{\rho}_{12,\mathrm{IV}}(t).$$

$$n_B(\varepsilon) = \frac{1}{e^{\varepsilon/k_BT} - 1},$$

is the Bose–Einstein distribution and ε is the (absolute) energy difference associated with the jump induced by $\hat{L}_\varepsilon$.

Let us assume the bath coupling strengths linear in energy [17]

$$\kappa(\varepsilon) = \left(\frac{C_g}{C_\Sigma}\right)^2 \frac{R}{Z_{\mathrm{sys}}}\frac{\varepsilon}{\hbar}.$$

Lindblad Master Equation

Let us assume that thermalization requires the global Lindblad equation.

In contrast, the local Lindblad equation may be used to describe the decoherence in the system.

The jump operators for the global master equation are given [17, 27]

$$\hat{L}_\varepsilon = \sum_{\lambda - \lambda' = \varepsilon} |E_{\lambda'}\rangle \langle E_{\lambda'}| \hat{A} |E_\lambda\rangle \langle E_\lambda| ,$$

where $\hat{A}$ is the collapse operator for the local Lindblad equation.

[17] P.P. Hofer, et al. New J. Phys. 19, 123037 (2017).

[27] M. Cattaneo, G. L. Giorgi, S. Maniscalco, & R. Zambrini, New J. Phys. 21, 113045 (2019).

Lindblad Equation: Jump Operators

Let us assume that the system cools for the cycle, so we need to connect it with the hot heat bath.

Then, $\hat{A}_h = \mathbb{I} \otimes \hat{\sigma}_-$ and $\hat{A}_h = \hat{\sigma}_- \otimes \mathbb{I}$ ($\hat{A}_h^\dagger = \mathbb{I} \otimes \hat{\sigma}_+$ and $\hat{A}_h^\dagger = \hat{\sigma}_+ \otimes \mathbb{I}$) are the collapse operators for the local Lindblad equation as both qubits are coupled to the thermal bath [17].

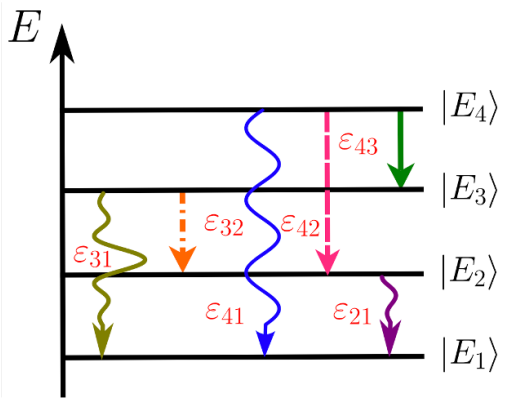

Figure 8: Energy level diagram with possible energy transitions.

[17] P.P. Hofer, et al. New J. Phys. 19, 123037 (2017).

Lindblad Equation

$$\dot{\rho}_{12,\mathrm{IV}}(t) = -\frac{i}{\hbar}[\rho_{12,\mathrm{IV}}(t), \hat{H}_{sys}] + \sum_{n=1}^{2} \Gamma_{0n}\mathcal{D}[\hat{C}_n]\hat{\rho}_{12,\mathrm{IV}}(t) +$$

$$2\Gamma_{n,\varphi}\mathcal{D}[\hat{C}_n{}^{\dagger}\hat{C}_n]\hat{\rho}_{12,\mathrm{IV}}(t) + \sum_{\varepsilon} \Gamma_{\varepsilon}\mathcal{D}[\hat{L}_{\varepsilon}^{\dagger}]\hat{\rho}_{12,\mathrm{IV}}(t) + \overline{\Gamma}_{\varepsilon}\mathcal{D}[\hat{L}_{\varepsilon}]\hat{\rho}_{12,\mathrm{IV}}(t).$$

Here, $C_1 = \mathbb{I} \otimes \sigma_z$ and $C_2 = \sigma_z \otimes \mathbb{I}$ for the ZZ-coupling.

Because of the circuit's insensitivity to charge noise [6], we may neglect pure dephasing rate Γ_{φ} [25].

[6] Y. Wang, Z. Wang, & C. Sun, Phys. Rev. B 72, 172507 (2005).

[25] A. Blais, A. L. Grimsmo, S. M. Girvin, & A. Wallraff, Rev. Mod. Phys. 93, 025005 (2021).